


Removal of Disperse Orange and Disperse Blue dyes present in textile mill effluent using zeolite synthesized from cenospheres

Markandeya^a, Sheo Prasad Shukla^b and Arun Lal Srivastav^{c,*} 

^a Ex-Department of Civil Engineering, Indian Institute of Technology (BHU), Varanasi 221005, India

^b Rajkiya Engineering College, Banda 210201, India

^c Chitkara University School of Engineering and Technology, Chitkara University, Himachal Pradesh 174103, India

*Corresponding author. E-mail: arun.srivastav@chitkarauniversity.edu.in; arunitbhu2009@gmail.com

 ALS, 0000-0003-0238-7395

ABSTRACT

In this research, an efficient, ecofriendly method of using coal fly ash in the form of zeolite to treat wastewater containing dyes was studied. Response surface methodology involving Box–Behnken design was applied to a batch process to evaluate the effect of process parameters such as contact time, dye concentration, agitation speed, pH, and adsorbent dosage onto zeolite. Disperse Orange 25 (DO) dye showed a maximum of 96% removal under optimal conditions of contact time of 119 min, dye concentration of 38.00 mg/L, agitation speed of 158 rpm, pH of 6.10, and adsorbent dosage of 0.67 g/L, whereas 95.23% of Disperse Blue 79:1 (DB) dye removal was observed at adsorbent dose of 1.05 g/L, dye concentration of 26.72 mg/L, agitation speed of 145 rpm, pH of 5.68, and contact time of 122 min. It was concluded that cenosphere-derivatized zeolite adsorbent is efficient, ecofriendly, and economical and has high potential for the removal of DO and DB dyes from aqueous solutions.

Key words: Box–Behnken design, cenospheres, disperse dyes, response surface methodology

HIGHLIGHTS

- Modified cenosphere-based zeolite used for dye removal from wastewater.
- Box–Behnken design used to optimize the optimum conditions for dye removal from wastewater.
- Maximum Disperse Orange 25 and Disperse Blue 79:1 removal was 96% and 95.23%, respectively.
- Derivatized zeolite is ecofriendly and economical for dye removal from wastewater.

INTRODUCTION

Dyes are one of the most hazardous contaminants released in to the environment and can be teratogenic, carcinogenic, and mutagenic to humans and other organisms if untreated dye-containing wastewater is discharged into water bodies (Markandeya *et al.* 2017d; Pandey *et al.* 2017). Dyes in wastewater cause color changes in the receiving water body, which is a sign of contamination due to dissolved metal ions, pigments, and other organic elements, and they also affect the aesthetics of the surrounding area (Dhiman *et al.* 2017b; Mohammed *et al.* 2020). Dyes can be naturally and synthetically derived and are commonly used in coloring of paper, electroplating materials, plastic, leather, cosmetic, food, pharmaceuticals, and textile mills (Singh *et al.* 2019; Ahmad *et al.* 2020). However, only textile mills produce very high levels of dye and floating solid materials containing effluent (Ojha & Markandeya 2016; Thirunavukkarasu & Nithya 2020). Therefore, removal of dye stuff from wastewater is necessary to ensure the safety of drinking water sources.

Disperse dyes are widely used for the coloring of polyesters, nylon, natural fibres, and acetate in the textile sector because of their bonding stability under different physical parameters (Kisku *et al.* 2015). Different chemical groups may be present in varying amounts, such as diazo dyes (10%), mono azo dyes (50%), styryl dyes (03%), anthraquinonoid dyes (25%), methine dyes (3%), acrylene benzimidazol (3%), amino naphthyl amide (1%), quinonaphthalon dyes (3%), and napthoquinone imine (1%) (Markandeya *et al.* 2017a). Azo dyes are the largest group of disperse dyes because they generate large numbers of molecular combinations, which results in a variety of dyes, and they also have a simple and low cost of production process compared to the expensive anthraquinone dyes (Markandeya *et al.* 2018). However, they have a complex aromatic fused

This is an Open Access article distributed under the terms of the Creative Commons Attribution Licence (CC BY-NC-ND 4.0), which permits copying and redistribution for non-commercial purposes with no derivatives, provided the original work is properly cited (<http://creativecommons.org/licenses/by-nc-nd/4.0/>).

structure that inhibits photosynthesis in aquatic plants (El-Shamy 2020). In many scientific studies, contact allergy has been reported after the use of synthetic textile dyes. In 1884 after the introduction of new synthetic organic dyes for dyeing fibres, numerous problems were reported such as skin eruptions caused by wearing dyed clothes (Markandeya *et al.* 2017b, 2017c). Further investigation revealed that dermatitis was associated with dyes and not by nylon (Markandeya *et al.* 2015b; Dhiman *et al.* 2017a). It is therefore imperative to develop methods of removing the dyes from wastewater in an efficient, ecofriendly, and economic way. Carvalho *et al.* (2011) studied adsorption of indigo carmine from the aqueous solutions using zeolite adsorbents. They developed zeolite using hydrothermal treatment with sodium hydroxide solution. The maximum adsorption capacity was found to be 1.23 mg/L. Lee *et al.* (2000) and Solanki *et al.* (2010) also used zeolite for the removal of wastewater impurities, but the adsorption capacity in zeolite was very low.

Statistical optimization of experimental conditions was carried out for the removal of dyes using zeolite derivatized from cenospheres. Response surface methodology (RSM) was used to reduce the total number of experiments and optimize the operating variables (Jawad *et al.* 2020e, 2021). RSM can enhance and optimize numerous process parameters and identify relative significances even in complex interactions (Markandeya *et al.* 2015a; Tiwari *et al.* 2015). It can establish favorable operational conditions for the process under investigation. RSM also offers many advantages like lowered process variability, increased percentage yield, and suitable confirmation of output response for both target and nominal achievements (Jawad *et al.* 2020a, 2020b, 2020c; Surip *et al.* 2020). The statistical design of the experiments determines which factors have the most effect on the response (percentage dye removal) (Jawad & Abdulhameed 2020a; Malek *et al.* 2020).

RSM is a sequential procedure that helps to quickly and efficiently identify optimum conditions (Tiwari *et al.* 2013; Reghioua *et al.* 2021b). Although statistical design of experiment has been mostly used in the optimization of industrial processes with multiple parameters (Haq *et al.* 2018), it has rarely been applied to adsorption processes (Jawad & Abdulhameed 2020b; Jawad *et al.* 2020d; Reghioua *et al.* 2021a). There is scope to determine the potential of statistical design in adsorption studies. The objective of this study was to determine a region of vector space in which operating requirements are satisfied for the removal of dyes using zeolite derivatized by cenospheres from wastewater in an efficient, ecofriendly, and economic manner.

MATERIALS AND METHODS

The molecular weight (g/mol) of Disperse Orange 25 (DO, C₁₇H₁₇N₅O₂) and Disperse Blue 79:1 (DB, C₂₃H₂₅BrN₆O₁₀) dyes was 323.35 and 625.38, respectively, and λ_{\max} (nm) was 470 and 570, respectively.

Synthesis of zeolite from modified cenospheres

Zeolite was prepared from modified cenospheres to enhance the adsorption capacity. Coal fly ash was modified as per the method described by Markandeya *et al.* (2017c) and (USEPA 1990) to obtain the modified cenospheres. The modified cenospheres were mixed with alumina and calcium hydroxide in the ratio of 1:6:1 (w/w). To make slurry (A) with a concentration of 2 weight%, the mixture was mixed with Milli-Q water. Then the slurry (A) was mixed with sodium bicarbonate as the binding mixture in different proportions in four separate columns:

- slurry (A);
- slurry (A) and sodium bicarbonate (10:1 w/w);
- slurry (A) and sodium bicarbonate (10:2 w/w);
- slurry (A) and sodium bicarbonate (10:3 w/w).

Sodium bicarbonate was used as a binding material to prevent percolation and the ratio 10:2 (w/w) of slurry (A) and sodium bicarbonate produced the best result. The zeolite produced from modified cenospheres was used as an adsorbent for this study (Figure 1).

Experimental design

RSM is an empirical technique used to identify operating variables for the optimum removal of contaminants or impurities from wastewater. The variables affecting the percentage removal of dyes were investigated using the Box–Behnken design (BBD). The experimental design was carried out using Design-Expert software, v 11 (Stat-Ease Inc., USA). All experiments were performed in batch system using a 250-mL reactor containing 100 mL of DO or DB dye solution. The variable input parameters were contact time from 60 to 140 min for DO and 80 to 160 min for DB, dye concentration from 20 to 60 mg/L, agitation speed from 100 to 180 rpm, pH values from 4 to 8 for DO and 4 to 10 for DB dyes, and adsorbent dosage

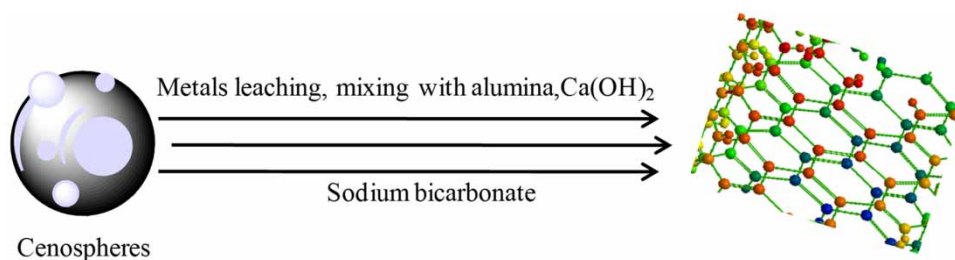


Figure 1 | Graphical representation of zeolite synthesized from modified cenospheres.

values from 0.2 to 1.0 g/L for DO and 0.4 to 1.2 g/L for DB dyes. Selection of process parameters was done on the basis of batch experiments conducted previously (Markandeya *et al.* 2017d). Five independent parameters for optimization were contact time (A), dye concentration (B), agitation speed (C), pH (D), and adsorbent dosage (E). The main processes involved in the optimization of multiple variables included statistically designing the experiment, estimating the coefficient, analyzing the response, and checking the suitability of the model (Box & Behnken 1960; Jaafari *et al.* 2020).

The range of each inconsistent parameter was coded to between -1 and $+1$, whereas the middle value was 0 (Desai & Shrivastava 2008). Moreover, the real values of all inconsistent parameters were converted into their corresponding coded values using Equation (1):

$$Z_i = \frac{X_i - X_0}{\Delta X_i} \quad (1)$$

where Z_i is the dimensionless coded value of i th independent variable, X_0 is the uncoded value of the i th independent variable at the center point, X_i is the uncoded value of the i th independent variable, and ΔX_i is the value change in the step.

In RSM, it is important to identify a suitable approximation for the true functional relationship between y and the set of independent variables. A lower order polynomial equation relating the independent parameters was used. For the linear function response of independent variables, the approximate function followed the first-order model according to Equation (2):

$$y = \beta_0 + \beta_1 X_1 + \beta_2 X_2 + \beta_3 X_3 + \dots + \beta_k X_k + \varepsilon \quad (2)$$

In a curvature system, a higher degree polynomial equation was required, which can be calculated using Equation (3):

$$y = \beta_0 + \sum_{i=1}^k \beta_i X_i + \sum_{i=1}^k \beta_{ii} X_i^2 + \sum_{i < j}^k \beta_{ij} X_i X_j + \varepsilon \quad (3)$$

where y is the predicted percentage removal of dyes, β_i is the linear coefficient of the input parameter X_i , β_0 is the constant coefficient, β_{ii} is i th quadratic coefficient of X_i , β_{ij} is the interaction coefficient between X_i and X_j and ε is error in the model.

For this study, the inconsistent parameters of the whole process were coded as A, B, C, D, and E and Equation (2) can be rewritten as:

$$y = \beta_0 + \beta_1 A + \beta_2 A^2 + \beta_3 B + \beta_4 B^2 + \beta_5 C + \beta_6 C^2 + \beta_7 D + \beta_8 D^2 + \beta_9 E + \beta_{10} E^2 + \beta_{11} AB + \beta_{12} AC + \dots + \beta_{46} DE + \varepsilon \quad (4)$$

The model coefficients (β_i) are determined and used for predicting response values for different combinations of coded values of the variables.

RESULTS AND DISCUSSION

Characterization of zeolite

This study analyzed and quantified the characteristics and morphological properties of the zeolite adsorbent. The, roughness/smoothness of the surface and other different properties of the cenospheres and zeolite are shown in Figure 2a and 2b,

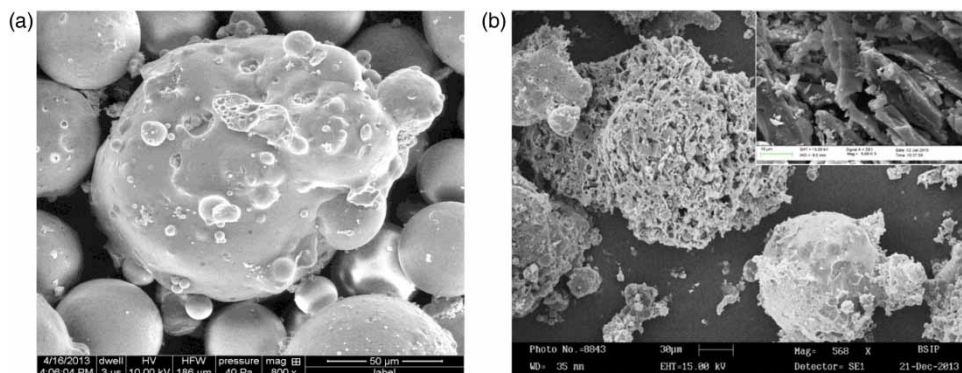


Figure 2 | SEM photomicrograph of (a) cenospheres and (b) zeolite.

respectively. Cenospheres are uniform spherical aggregates with a rough and porous texture which provides high surface area to mass ratio, thereby facilitating the adsorption of dye molecules. The insets in [Figure 2b](#) (scaled at $10\ \mu\text{m}$) show scanning electron microscopy (SEM) images of zeolite at higher magnification and represents aggregates of zeolite crystals with defined grain boundaries ([Dhiman et al. 2017b](#)). Energy-dispersive X-ray (EDX) spectroscopy plots in [Figure 3](#) shows that zeolite (b) contained more aluminum, calcium, and silica than the metal-leached-out-cenospheres (a).

Brunauer–Emmett–Teller analysis showed that the surface area was $2,832.08\ \text{m}^2/\text{g}$ and pore volume was $8.37\ \text{cm}^3/\text{g}$ at pores less than $2,153\ \text{Å}$ at P/Po, 0.9910, whereas pore size was $698.32\ \text{Å}$ Barrett–Joyner–Halenda average adsorption pore diameter of $4\ \text{V/A}$ ([Kacan 2016](#)).

Spectral analyses of cenospheres and zeolite using attenuated total reflection–Fourier transform infrared (ATR–FTIR) spectroscopy are shown in [Figure 4](#). Cenospheres (a) displayed two peaks at $1,053$ and $798\ \text{cm}^{-1}$ analogous to an asymmetric and symmetric marking of M–O–M (M = Si/Al). However, some intense peaks were observed due to desired modification on cenospheres. [Jain et al. \(2013\)](#) also found such peaks after modification of coal fly ash, which matches this study. Moreover, a peak at $1,463\ \text{cm}^{-1}$ in zeolite spectrum ([Figure 4b](#)) demonstrated the presence of sodium bicarbonate. [Mason et al. \(2006\)](#) also found sodium bicarbonate at the same peak length. The presence of the weak band at $3,463\ \text{cm}^{-1}$ is related to O–H stretching of water molecules.

The size of the particles was in the micrometer range and their diameter was heterogeneous ([Figure 5\(a\)](#)). This variation can be explained by non-uniform distribution of raw cenospheres ([Figure 6\(a\)](#)). The smallest particle size ($70\text{--}300\ \text{nm}$) determined by TEM is shown in [Figure 5\(b\)](#).

Particle size distribution plot shown in [Figure 6\(a\)](#) demonstrate that the most common granular size was $30\text{--}60\ \mu\text{m}$, whereas [Figure 6\(b\)](#) of formed zeolite shows that the most common granule size was in the range of $10\text{--}50\ \mu\text{m}$.

Adsorption study and regression model

We applied three isotherms – Langmuir, Freundlich, and Temkin–and found that Langmuir isotherm better correlated compared to the others for the adsorption of dye onto the zeolite surface. The monolayer maximum adsorption capacity was found to be $125\ \text{mg/g}$ and $109.8\ \text{mg/g}$ for DO and DB dyes, respectively. The values of $R_L = 0.0909$ and 0.1656 also revealed

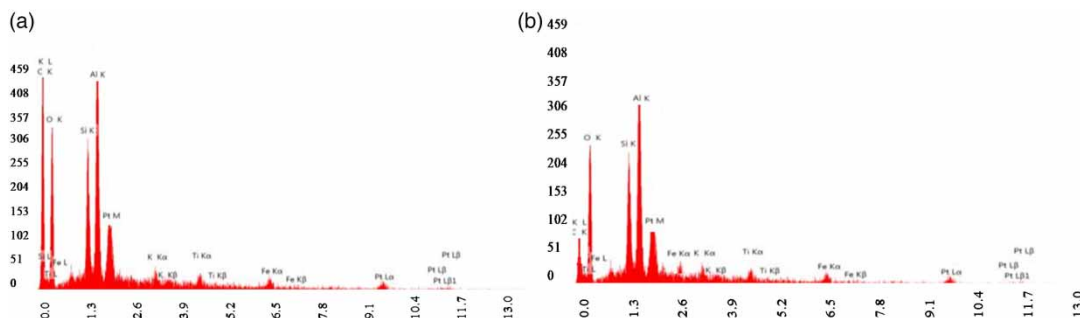


Figure 3 | EDX plots of (a) cenospheres and (b) zeolite.

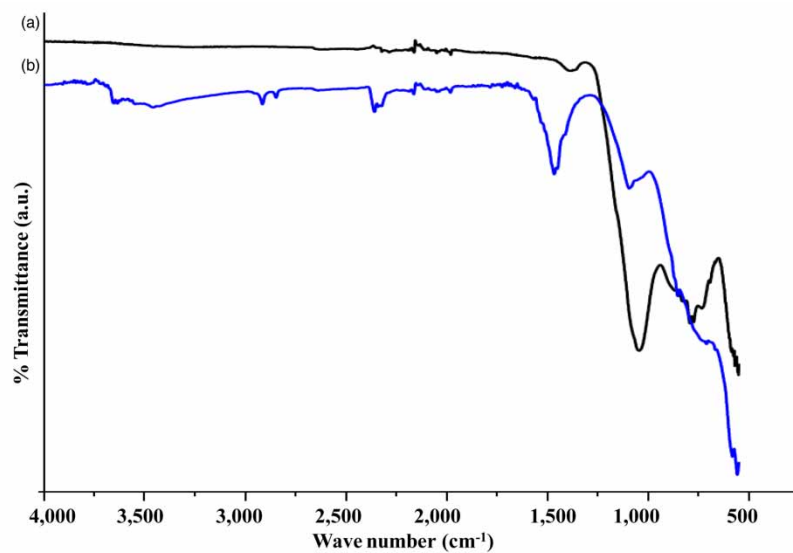


Figure 4 | ATR-FTIR spectra of (a) cenospheres and (b) synthesized zeolite.

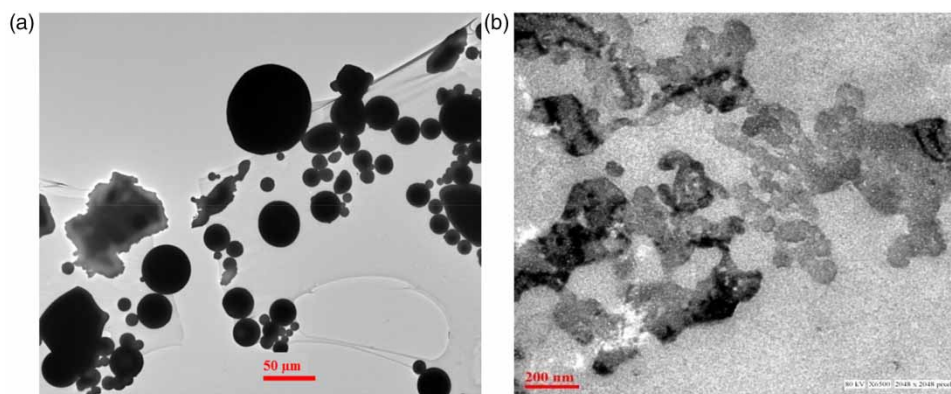


Figure 5 | TEM for (a) cenospheres and (b) zeolite granules.

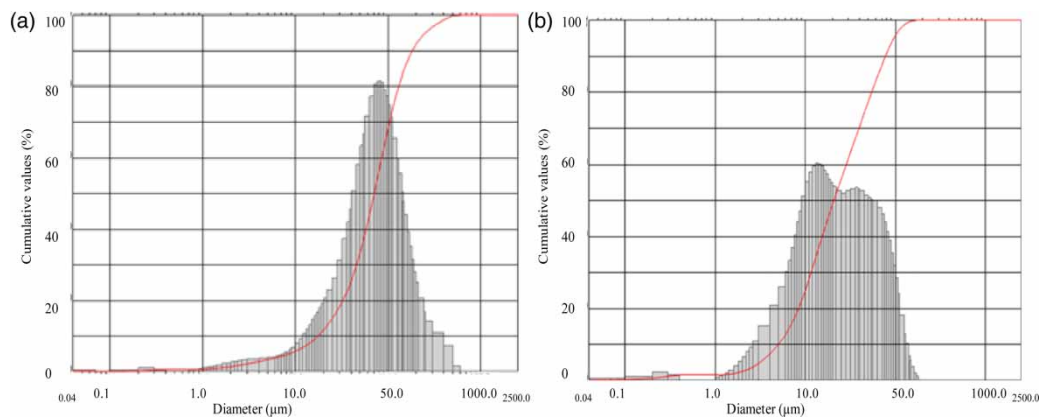


Figure 6 | Particle size distribution profile of (a) cenospheres and (b) zeolite granules.

a favorable isotherm for DO and DB dyes, respectively. Based on R^2 values of pseudo-first-order and second-order kinetic models, the adsorption process in this study follows the pseudo-second-order kinetic model as it gives a maximum value of R^2 (Markandeya *et al.* 2017b).

RSM-based BBD was used to optimize conditions for maximum uptake of dyes onto the zeolite surface. A statistical model was developed using quantitative data obtained from experiments using Equation (4) and transforming this equation in terms of coded and actual factors as shown in Equations (5)–(8):

Final equation for DO dye in terms of coded factors:

$$\begin{aligned} \% \text{ Removal (y)} = & +93.0 + 3.52 \times A - 2.52 \times B + 2.01 \times C + 2.61 \times D \\ & + 7.61 \times E + 1.0 \times A \times B + 0.26 \times A \times C + 0.05 \times A \times D \\ & - 0.38 \times A \times E - 0.04 \times B \times C + 0.75 \times B \times D \\ & + 0.56 \times B \times E - 1.88 \times C \times D + 1.73 \times C \times E - 1.0 \times D \times E \\ & - 2.61 \times A^2 - 5.50 \times B^2 - 1.94 \times C^2 - 11.41 \times D^2 - 8.81 \times E^2 \end{aligned} \quad (5)$$

Final equation for DB dye in terms of actual factors:

$$\begin{aligned} \% \text{ Removal} = & -124.7964 + 0.33521 \times \text{contact time} + 0.7018 \times \text{dye concentration} \\ & + 0.4532 \times \text{agitation speed} + 38.7594 \times \text{pH} + 77.0859 \times \text{adsorbent dosage} \\ & + 1.25 \times 10^{-3} \times \text{contact time} \times \text{dye concentration} + 1.5625 \times 10^{-4} \\ & \times \text{contact time} \times \text{agitation speed} + 6.25 \times 10^{-4} \times \text{contact time} \times \text{pH} \\ & - 0.0234 \times \text{contact time} \times \text{adsorbent dosage} - 5.3125 \times 10^{-5} \\ & \times \text{dye concentration} \times \text{agitation speed} + 0.018750 \times \text{dye concentration} \times \text{pH} \\ & + 0.0697 \times \text{dye concentration} \times \text{adsorbent dosage} \\ & - 0.023438 \times \text{agitation speed} \times \text{pH} + 0.1078 \times \text{agitation speed} \times \text{adsorbent dosage} \\ & - 1.2500 \times \text{pH} \times \text{adsorbent dosage} - 1.6286 \times 10^{-3} \times \text{contact time}^2 \\ & - 0.013744 \times \text{dye concentration}^2 - 1.2156 \times 10^{-3} \times \text{agitation speed}^2 \\ & - 2.85313 \times \text{pH}^2 - 55.07292 \times \text{adsorbent dosage}^2 \end{aligned} \quad (6)$$

Final equation for DO dye in terms of coded factors:

$$\begin{aligned} \% \text{ Removal (y)} = & +89.68 + 3.36 \times A - 6.55 \times B + 2.31 \times C + 3.25 \times D \\ & + 9.33 \times E + 0.46 \times A \times B + 2.08 \times A \times C - 2.88 \times A \times D - 1.19 \times A \times E \\ & + 1.81 \times B \times C + 0.046 \times B \times D + 1.77 \times B \times E - 0.63 \times C \times D - 0.97 \times C \times E \\ & - 4.51 \times D \times E - 1.91 \times A^2 - 3.84 \times B^2 - 1.63 \times C^2 - 7.92 \times D^2 - 5.57 \times E^2 \end{aligned} \quad (7)$$

Final equation for DB dye in terms of actual factors:

$$\begin{aligned} \% \text{ Removal} = & -118.7328 + 0.4408 \times \text{contact time} - 0.1292 \times \text{dye concentration} \\ & + 0.1921 \times \text{agitation speed} + 35.2561 \times \text{pH} + 121.5143 \times \text{adsorbent dosage} \\ & + 5.787 \times 10^{-4} \times \text{contact time} \times \text{dye concentration} + 1.3021 \times 10^{-3} \\ & \times \text{contact time} \times \text{agitation speed} - 0.0360 \times \text{contact time} \times \text{pH} - 0.0747 \\ & \times \text{contact time} \times \text{adsorbent dosage} + 2.2569 \times 10^{-3} \\ & \times \text{dye concentration} \times \text{agitation speed} + 1.1574 \times 10^{-3} \times \text{dye concentration} \times \text{pH} \\ & + 0.2216 \times \text{dye concentration} \times \text{adsorbent dosage} - 7.8125 \times 10^{-3} \times \text{agitation speed} \\ & \times \text{pH} - 0.0607 \times \text{agitation speed} \times \text{adsorbent dosage} - 5.6424 \times \text{pH} \\ & \times \text{adsorbent dosage} - 1.1934 \times 10^{-3} \times \text{contact time}^2 - 9.6021 \times 10^{-3} \\ & \times \text{dye concentration}^2 - 1.0193 \times 10^{-3} \times \text{agitation speed}^2 - 1.9789 \times \text{pH}^2 \\ & - 34.8368 \times \text{adsorbent dosage}^2 \end{aligned} \quad (8)$$

The process variables and experimental responses for DO and DB dyes were calculated. Analysis of variance (ANOVA) for predicted response surface quadratic model was also calculated using Design-Expert software and the results are presented in Tables 1 and 2.

F-test and correlation coefficient (R^2) were used to check significance level. Model terms were evaluated with 95% confidence level using p -values. 3D plots were developed for removal of DO and DB dyes.

The F-value 12.67 implies that the model for the removal of DO dye is significant. There is only a 0.01% chance that large F-values could occur due to noise. The values of $\text{Prob} > F < 0.05$ confirmed that the model fits significantly. In this case, the significant model terms are A, B, C, D, E, A^2 , B^2 , D^2 , and E^2 and values greater than 0.1 indicate that the model terms were not significant (Table 1). If there are a number of insignificant model terms (without including those required to support hierarchy), the model can be reduced.

The model F-values of 11.75 imply that the model developed for DB dye fitted significantly. The values of $\text{Prob} > F < 0.05$ clearly indicate that the model terms were significant. The significant model terms are A, B, C, D, E, DE, B^2 , D^2 , and E^2 and values greater than 0.1 indicate that these model terms are not significant (Table 2). Moreover, the lack-of-fit F-value of 1,397.58 specifies that the lack-of-fit was significant. There is a very small probability (only a 0.01%) that a large lack-of-fit F-value could occur due to noise. Table 3 presents the model fit summary of the quadratic models developed for both dyes.

For DO dye, the value $\text{Pred } R^2$ was 0.6409, which is better correlated with the value $\text{Adj } R^2$ of 0.8384. If the ratio of signal (observation) to noise (error) is greater than 4, then it is desirable. The present ratio of 14.084 indicates an adequate signal, and therefore this model can be used to navigate the design space successfully.

Table 1 | ANOVA for the removal of DO dye of response surface quadratic model

Variable source	Sum of mean ²	DF	Value ²	F	p-value	Remarks
Model	2,988.80	20	149.44	12.67	<0.0001	Significant
A: contact time	198.11	1	198.11	16.80	0.0004	Significant
B: pH	108.68	1	108.68	9.22	0.0055	Significant
C: agitation speed	64.92	1	64.92	5.51	0.0272	Significant
D: adsorbent dosage	927.66	1	927.66	78.67	<0.0001	Significant
E: dye concentration	101.30	1	101.30	8.59	0.0071	Significant
AB	4.00	1	4.00	0.34	0.5655	Insignificant
AC	0.25	1	0.25	0.02	0.8854	Insignificant
AD	0.01	1	0.010	8.480×10^{-4}	0.9770	Insignificant
AE	0.56	1	0.56	0.05	0.8289	Insignificant
BC	7.225×10^{-5}	1	7.225×10^{-5}	6.127×10^{-4}	0.9804	Insignificant
BD	2.25	1	2.25	0.19	0.6660	Insignificant
BE	1.24	1	1.24	0.11	0.7481	Insignificant
CD	14.06	1	14.06	1.19	0.2852	Insignificant
CE	11.90	1	11.90	1.01	0.3247	Insignificant
DE	4.00	1	4.00	0.34	0.5655	Insignificant
A^2	59.26	1	59.26	5.03	0.0341	Significant
B^2	263.76	1	263.76	22.37	<0.0001	Significant
C^2	33.02	1	33.02	2.80	0.1067	Insignificant
D^2	1,136.69	1	1,136.69	96.39	<0.0001	Significant
E^2	677.63	1	677.63	57.46	<0.0001	Significant
Residual	294.81	25	11.79	–	–	Insignificant
Lack-of-fit	294.81	20	14.74	–	–	Insignificant
Pure error	0.00	5	0.00	–	–	Insignificant
Cor total	3,283.60	45	–	–	–	Insignificant

Table 2 | ANOVA for the removal of DB dye of response surface quadratic model

Variable source	Sum of mean ²	DF	Value ²	F	p-value	Remarks
Model	3,379.56	20	168.98	11.75	<0.0001	Significant
A: contact time	180.32	1	180.32	12.54	0.0016	Significant
B: pH	687.36	1	687.36	47.80	<0.0001	Significant
C: agitation speed	85.31	1	85.31	5.93	0.0223	Significant
D: adsorbent dosage	168.94	1	168.94	11.75	0.0021	Significant
E: dye concentration	1,392.40	1	1,392.40	96.82	<0.0001	Significant
AB	0.86	1	0.86	0.06	0.8091	Insignificant
AC	17.36	1	17.36	1.21	0.2824	Insignificant
AD	33.22	1	33.22	2.31	0.1411	Insignificant
AE	5.71	1	5.71	0.40	0.5344	Insignificant
BC	13.04	1	13.04	0.91	0.3501	Insignificant
BD	8.57×10^{-5}	1	8.57×10^{-5}	5.96×10^{-4}	0.9807	Insignificant
BE	12.58	1	12.58	0.87	0.3587	Insignificant
CD	1.56	1	1.56	0.11	0.7444	Insignificant
CE	3.78	1	3.78	0.26	0.6126	Insignificant
DE	81.50	1	81.50	5.67	0.0252	Significant
A ²	31.82	1	31.82	2.21	0.1494	Insignificant
B ²	128.75	1	128.75	8.95	0.0062	Significant
C ²	23.22	1	23.22	1.61	0.2156	Insignificant
D ²	546.84	1	546.84	38.02	<0.0001	Significant
E ²	271.14	1	271.14	18.85	0.0002	Significant
Residual	359.53	25	14.38	–	–	Insignificant
Lack-of-fit	359.46	20	17.97	1,397.58	<0.0001	Insignificant
Pure error	0.06	5	0.01	–	–	Insignificant
Cor total	3,739.08	45	–	–	–	Insignificant

Table 3 | Summary for the quadratic model statistics for DO and DB dyes

Dyes	Standard deviation	Mean	Coefficient of variation	Prediction sum of squares	R ²	Adjusted R ²	Predicted R ²	Adeq. precision
DO	3.43	82.47	4.16	1,179.23	0.9102	0.8384	0.6409	14.084
DB	3.79	82.42	4.60	1,437.94	0.9038	0.8269	0.6154	13.768

For DB, the value Pred R² was 0.6154, which is in reasonable agreement with the value Adj R² of 0.8269. Adeq precision also measures the signal (observation) to noise (error) ratio and, in this case, the value 13.768 indicates adequacy of signal. Therefore, this model can be effectively used to navigate the design space.

Validation of model

Validation of model was performed using different combinations of five variables: contact time, pH, agitation speed, adsorbent dosage, and dye concentration for DO and DB dyes. The predicted and experimental values of the model were compared to determine validity of the models (Tables 4 and 5).

The optimization process was accomplished using numerical node under optimized conditions. During optimization, five adsorption governing factors (pH, contact time, agitation speed, dosage, and initial dye concentration) were adjusted and maximum removals were reported for both DO and DB dyes. The Design-Expert software integrated individual factors at tunable levels.

Table 4 | Corresponding values of the response parameters and actual values of the independent parameters sets for DO dye

Experimental run	A: contact time (min)	B: pH	C: agitation speed (rpm)	D: adsorbent dosage (g/L)	E: dye concentration (mg/L)	Removal (%)	
						Predicted	Experimental
1	130.48	5.99	129.71	0.72	33.28	93.70	91.67
2	133.73	5.93	173.73	0.66	37.76	95.82	94.05
3	118.53	5.77	153.95	0.83	36.98	96.13	94.96
4	95.65	6.29	170.14	0.79	43.09	94.61	92.81
5	130.61	6.05	138.55	0.85	36.75	95.32	95.59
6	119.00	6.10	158.00	0.67	38.00	96.00	94.65

Table 5 | Corresponding values of the response parameters and actual values of the independent parameters sets for DB dye

Experimental run	A: contact time (min)	B: pH	C: agitation speed (rpm)	D: adsorbent dosage (g/L)	E: dye concentration (mg/L)	Removal (%)	
						Predicted	Experimental
1	110.00	6.56	137.00	1.05	24.10	91.22	90.05
2	130.00	5.96	146.00	0.93	27.27	95.00	95.98
3	097.00	6.29	131.00	1.06	23.71	93.61	92.21
4	149.00	5.19	134.00	1.17	29.69	88.05	86.15
5	119.00	5.76	173.00	0.97	20.82	93.32	92.52
6	122.00	5.68	145.00	1.05	26.72	95.23	94.11

To achieve further understanding regarding effects of the independent parameters and their interactions with dependent parameters (removal), 3D response surface plots for the measured responses were made based on the quadratic models. 3D response surfaces indicate that the interaction between the corresponding parameters are negligible. An elliptical or saddle shape of the contour plots indicates a significant interaction between two variables (Liu & Chiou 2005). In Figure 7, the upper horizontal axis represents the dependent variable and the almost parallel contour lines suggest that there is no significant interaction between the variables.

3D response surface plots and 3D contour plots (Figure 7(a) and 7(b)) for the removal of both dyes show that zeolite (adsorbent) was a function of dye concentration and contact time. The percentage removals of DO and DB dyes initially increased rapidly as the contact time increased and decreased as the contact time decreased. As the dye concentrations increased, the percentage removal of both dyes decreased within the respective experimental ranges. However, DO dye was found to be more prominent compared to the DB dye on contact time and dye concentration (Figure 7(a) and 7(b)). This may be due to the presence of more unstable chemicals in the matrix of the DO dye (Nandi *et al.* 2009). Shukla *et al.* (2014) also found the same results. It has also been observed that the removal of both dyes increases with an initial increase in dye concentrations (10 to 40 mg/L), but an increase from 40 to 60 mg/L caused the removal of dye to decrease. This may be because of the relatively limited adsorption sites for higher dye concentrations, i.e., >50 mg/L.

Figure 7(c) and 7(d) presents the 3D response surface plots for the percentage removal of DO and DB dyes as a function of agitation speed and contact time. It is clear that the removal percentage increased with the increasing contact time, but there was no significant effect for agitation speed (Wang 2013). The curved portion of the Figure 7(c) and 7(d) indicates that there is almost no interactive influence of these two parameters on decolorization.

Figure 7(e) and 7(f) shows 3D response surface plots for decolorization as a function of pH and contact time. In this case, the removal percentage increased with increasing pH value (from pH 2 to 6) but decreased with a further increase in pH up to 8 (Yahia & Sellaoui 2020). The curved portion in Figure 7(e) and 7(f) indicates that for the removal of the dyes, there was good interaction between pH and contact time.

Figure 7(g) and 7(h) shows 3D response surface plots for decolorization as a function of adsorbent dosage and contact time. It can be seen that the percentage removal of both dyes increased with increasing adsorbent dosage. However, the removal of DO dye was greater compared to DB dye, as shown in Figure 7(g). The percentage removal increased as the adsorbent dosage

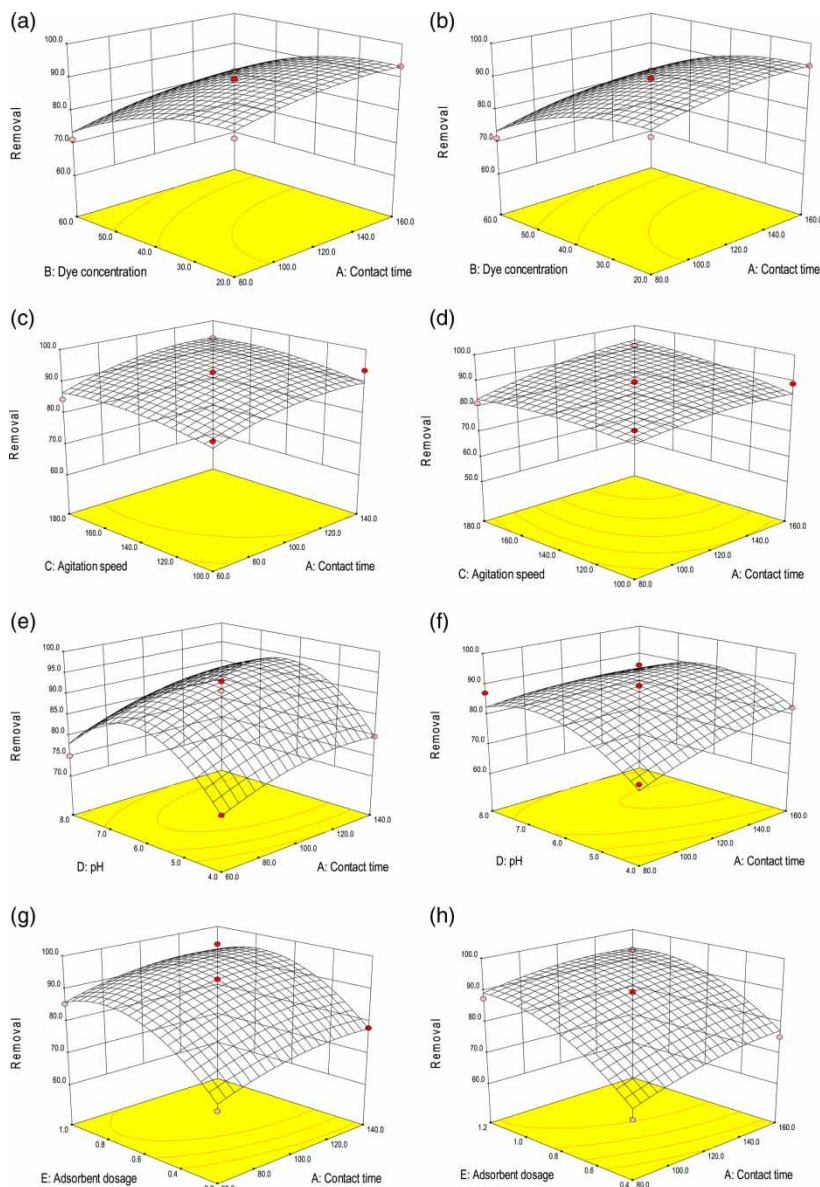


Figure 7 | 3D response surface plots for percentage of dye removal in relation to (a, b) concentration and contact time, (c, d) agitation speed and contact time, (e, f) pH and contact time, and (g, h) adsorbent dosage and contact time.

Table 6 | Comparison of maximum adsorption capacity

Adsorbent	Capacity (mg/g)	Dyes	References
Commercial zeolite	2.1	Crystal Violet	Shirani <i>et al.</i> (2014)
Natural zeolite	16.4	Methylene Blue	Han <i>et al.</i> (2009)
Commercial zeolite-A	22.0	Methylene Blue	Rida <i>et al.</i> (2013)
NaA zeolite	64.8	Methylene Blue	Sapawe <i>et al.</i> (2013)
Hierarchical zeolite Y	133.1	Methylene Blue	Ramezani <i>et al.</i> (2019)
Zeolite modified from CFA	1.23	Indigo Carmine	Carvalho <i>et al.</i> (2011)
Zeolite modified from cenospheres	125.0	DO	Present study
	109.8	DB	

increased from 0.2 to 1.0 g/L; however, at a lower dosage of 0.2 g/L, fewer dye molecules could reach the limited number of available adsorption sites, resulting in lower removal. Increasing adsorbent dosage to 1.0 g/L resulted in the increased removal due to more sites available for the uptake of both dyes (Zhang *et al.* 2020).

Cubical representations of modeling for the removal of both DO and DB dyes were determined and the maximum values of dye removal were 96.00% and 95.23%, respectively, at the optimized parameters for DO dye and DB dye.

The maximum adsorption capacity of the present adsorbent was compared with other zeolite (Table 6). It is clear that the present zeolite adsorbent has good potential for the removal of both dyes compared to other zeolites prepared using different materials. In this study, the adsorption capacities for DO and DB dyes were 125.0 mg/L and 109.8 mg/L, respectively.

CONCLUSIONS

This investigation was based on the removal of disperse dyes from colored wastewater using an optimization technique. The optimization technique was based on the batch process and focused on the interactions between various parameters: pH, contact time, agitation speed, adsorbent dosage, and dye concentration. Related R^2 values of 0.9102 and 0.9038 proved that predicted data fitted well with actual data for both dyes. Based on the optimized conditions, the maximum percentage removal of DO was 96.00% (contact time: 119 min, adsorbent dosage: 0.67 g/L, shaking speed: 158 rpm, pH 6.10), and for DB dye it was 95.23% (contact time: 122 min, adsorbent dosage: 1.05 g/L, shaking speed: 145 rpm, pH 5.68). It was also observed that zeolite can be used for efficient removal of disperse dyes. ANOVA and regression modeling showed that all the process parameters have values of Prob. $>F < 0.05$, which indicates that the RSM-based BBD model was significant in the present study. The study also concluded that modified adsorbent zeolite has a high potential for use in the removal of dyes from colored wastewater.

ACKNOWLEDGEMENTS

The first author is highly grateful to Vibhuti Mishra for language correction. The work was financially supported by TEQIP II (TEQIP-II 22).

CONFLICT OF INTEREST

There is no conflict of interest.

DECLARATIONS

All authors have read and approved the manuscript.

DATA AVAILABILITY STATEMENT

All relevant data are included in the paper or its Supplementary Information.

REFERENCES

- Ahmad, M. A., Eusoff, M. A., Oladoye, P. O., Adegoke, K. A. & Bello, O. S. 2020 Statistical optimization of Remazol Brilliant Blue R dye adsorption onto activated carbon prepared from pomegranate fruit peel. *Chemical Data Collections* **28**, 100426. <https://doi.org/10.1016/j.cdc.2020.100426>.
- Box, G. E. & Behnken, D. W. 1960 Some new three level designs for the study of quantitative variables. *Technometrics* **2**, 455–475.
- Carvalho, T. E. M. D., Fungaro, D. A., Magdalena, C. P. & Cunico, P. 2011 Adsorption of indigo carmine from aqueous solution using coal fly ash and zeolite from fly ash. *Journal of Radioanalytical and Nuclear Chemistry* **289**, 617–626.
- Desai, T. N. & Shrivastava, R. L. 2008 Six Sigma—a new direction to quality and productivity management. In: *Proceedings of the World Congress on Engineering and Computer Science*, San Francisco, USA, pp. 1–6.
- Dhiman, N., Markandeya, Singh, A., Verma, N. K., Ajaria, N. & Patnaik, S. 2017a Statistical optimization and artificial neural network modeling for acridine orange dye degradation using in-situ synthesized polymer capped ZnO nanoparticles. *Journal of Colloid and Interface Science* **493**, 295–306.
- Dhiman, N., Markandeya, Fatima, F., Roy, S., Rout, P. K., Saxena, P. N. & Patnaik, S. 2017b Predictive modeling and validation of arsenite removal by one pot synthesized bioceramic buttressed manganese doped iron oxide nanoplateform. *RSC: Advances* **7**, 32866–32876.
- El-Shamy, A. G. 2020 An efficient removal of methylene blue dye by adsorption onto carbon dot @ zinc peroxide embedded poly vinyl alcohol (PVA/CZnO₂) nano-composite: a novel reusable adsorbent. *Polymer* **202**, 122565. <https://doi.org/10.1016/j.polymer.2020.122565>.

- Han, R., Wang, Y., Zhao, X., Wang, Y., Xie, F., Cheng, J. & Tang, M. 2009 Adsorption of methylene blue by phoenix tree leaf powder in a fixed-bed column: experiments and prediction of breakthrough curves. *Desalination* **245**, 284–297.
- Haq, I., Raj, A. & Markandeya. 2018 Biodegradation of Azure-B dye by *Serratia liquefaciens* and its validation by phytotoxicity, genotoxicity and cytotoxicity studies. *Chemosphere* **196**, 58–68.
- Jaafari, J., Barzanouni, H., Mazloomi, S., Farahani, N. A. A., Sharafi, K., Soleimani, P. & Haghghat, G. A. 2020 Effective adsorptive removal of reactive dyes by magnetic chitosan nanoparticles: kinetic, isothermal studies and response surface methodology. *International Journal of Biological Macromolecules* **164**, 344–355. <https://doi.org/10.1016/j.ijbiomac.2020.07.042>.
- Jain, M., Garg, V. & Kadirvelu, K. 2013 Cadmium(II) sorption and desorption in a fixed bed column using sunflower waste carbon calcium-alginate beads. *Bioresource Technology* **129**, 242–248.
- Jawad, A. H. & Abdulhameed, A. S. 2020a Facile synthesis of crosslinked chitosan-tripolyphosphate/kaolin clay composite for decolorization and COD reduction of remazol brilliant blue R dye: optimization by using response surface methodology. *Colloids and Surfaces A: Physicochemical and Engineering Aspects* **605**, 125329. <https://doi.org/10.1016/j.colsurfa.2020.125329>.
- Jawad, A. H. & Abdulhameed, A. S. 2020b Statistical modeling of methylene blue dye adsorption by high surface area mesoporous activated carbon from bamboo chip using KOH-assisted thermal activation. *Energy, Ecology and Environment* **5**, 456–469. <https://doi.org/10.1007/s40974-020-00177-z>.
- Jawad, A. H., Mohammed, I. A. & Abdulhameed, A. S. 2020a Tuning of fly ash loading into chitosan-ethylene glycol diglycidyl ether composite for enhanced removal of reactive red 120 dye: optimization using the Box–Behnken Design. *Journal of Polymers and the Environment* **28**, 2720–2733. <https://doi.org/10.1007/s10924-020-01804-w>.
- Jawad, A. H., Hum, N. N. M. F., Abdulhameed, A. S. & Ishak, M. A. M. 2020b Mesoporous activated carbon from grass waste via H_3PO_4 -activation for methylene blue dye removal: modelling, optimisation, and mechanism study. *International Journal of Environmental Analytical Chemistry*. <https://doi.org/10.1080/03067319.2020.1807529>
- Jawad, A. H., Abdulhameed, A. S., Malek, N. N. A. & ALOthman, Z. A. 2020c Statistical optimization and modeling for color removal and COD reduction of reactive blue 19 dye by mesoporous chitosan-epichlorohydrin/kaolin clay composite. *International Journal of Biological Macromolecules* **164**, 4218–4230. <https://doi.org/10.1016/j.ijbiomac.2020.08.201>.
- Jawad, A. H., Malek, N. N. A., Abdulhameed, A. S. & Razuan, R. 2020d Synthesis of magnetic chitosan-fly ash/ Fe_3O_4 composite for adsorption of reactive orange 16 dye: optimization by Box–Behnken design. *Journal of Polymers and the Environment* **28**, 1068–1082. <https://doi.org/10.1007/s10924-020-01669-z>.
- Jawad, A. H., Abdulhameed, A. S., Wilson, L. D., Syed-Hassan, S. S. A., ALOthman, Z. A. & Khan, M. R. 2020e High surface area and mesoporous activated carbon from KOH-activated dragon fruit peels for methylene blue dye adsorption: optimization and mechanism study. *Chinese Journal of Chemical Engineering*. <https://doi.org/10.1016/j.cjche.2020.09.070>
- Jawad, A. H., Abdulhameed, A. S., Wilson, L. D., Hanafiah, M. A. K. M., Nawawi, W. I., ALOthman, Z. A. & Khan, M. R. 2021 Fabrication of schiff's base chitosan-glutaraldehyde/activated charcoal composite for cationic dye removal: optimization using Response Surface Methodology. *Journal of Polymers and the Environment*. <https://doi.org/10.1007/s10924-021-02057-x>
- Kacan, E. 2016 Optimum BET surface areas for activated carbon produced from textile sewage sludges and its application as dye removal. *Journal of Environmental Management* **166**, 116–123.
- Kisku, G. C., Markandeya, Shukla, S. P., Singh, D. S. & Murthy, R. C. 2015 Characterization and adsorptive capacity of coal fly ash from aqueous solutions of disperse blue and disperse orange dyes. *Environmental Earth Sciences* **74**, 1125–1135.
- Lee, M., Yi, G., Ahn, B. & Roddick, F. 2000 Conversion of coal fly ash into zeolite and heavy metal removal characteristics of the products. *Korean Journal of Chemical Engineering* **17** (3), 325–331.
- Liu, H. L. & Chiou, Y. R. 2005 Optimal decolorization efficiency of reactive red 239 by UV/ TiO_2 photocatalytic process coupled with response surface methodology. *Chemical Engineering Journal* **112**, 173–179.
- Malek, N. N. A., Jawad, A. H., Abdulhameed, A. S., Ismail, K. & Hameed, B. H. 2020 New magnetic Schiff's base-chitosan-glyoxal/fly ash/ Fe_3O_4 biocomposite for the removal of anionic azo dye: an optimized process. *International Journal of Biological Macromolecules* **146**, 530–539. <https://doi.org/10.1016/j.ijbiomac.2020.01.020>.
- Markandeya, Singh, A., Shukla, S. P., Mohan, D., Singh, N. B., Bhargava, D. S., Shukla, R., Pandey, G., Yadav, V. P. & Kisku, G. C. 2015a Adsorptive capacity of sawdust for the adsorption of MB dye and designing of two-stage batch adsorber. *Cogent Environmental Science* **1**, 1075856.
- Markandeya, Shukla, S. P. & Kisku, G. C. 2015b Linear and non-linear kinetic modeling for the adsorption of disperse dye in a batch process. *Research Journal of Environmental Toxicology* **9** (6), 320–331.
- Markandeya, Shukla, S. P. & Dhiman, N. 2017a Characterization and adsorption of disperse dyes from wastewater onto cenospheres activated carbon composites. *Environmental Earth Sciences* **76**, 702–714.
- Markandeya, Shukla, S. P., Dhiman, N., Mohan, D., Kisku, G. C. & Roy, S. 2017b An efficient removal of disperse dye from wastewater using zeolite synthesized from cenospheres. *Journal of Hazardous, Toxic, and Radioactive Waste* **21** (4), 04017017.
- Markandeya, Shukla, S. P. & Mohan, D. 2017c Toxicity of disperse dyes and its removal from wastewater using various adsorbents: a review. *Research Journal of Environmental Toxicology* **11** (2), 72–89.
- Markandeya, Dhiman, N., Shukla, S. P. & Kisku, G. C. 2017d Statistical optimization of process parameters for removal of dyes from wastewater on chitosan cenospheres nanocomposite using response surface methodology. *Journal of Cleaner Production* **149**, 597–606.

- Markandeya, Dhiman, N., Shukla, S. P., Mohan, D., Kisku, G. C. & Patnaik, S. 2018 Comprehensive remediation study of disperse dyes containing wastewater by using environmental benign, low cost cenospheres nanosyntactic foam. *Journal of Cleaner Production* **182**, 206–216.
- Mason, T. G., Wilking, J., Meleson, K., Chang, C. & Graves, S. 2006 Nanoemulsions: formation, structure, and physical properties. *Journal of Physics: Condensed Matter* **18**, R635.
- Mohammed, I. A., Jawad, A. H., Abdulhameed, A. S. & Mastuli, M. S. 2020 Physicochemical modification of chitosan with fly ash and tripolyphosphate for removal of reactive red 120 dye: statistical optimization and mechanism study. *International Journal of Biological Macromolecules* **161**, 503–513. <https://doi.org/10.1016/j.ijbiomac.2020.06.069>.
- Nandi, B., Goswami, A. & Purkait, M. 2009 Adsorption characteristics of brilliant green dye on kaolin. *Journal of Hazard Materials* **161**, 387–395.
- Ojha, A. K. & Markandeya, 2016 Lignin decolorization and degradation of pulp and paper mill effluent by ligninolytic bacteria. *Iranica Journal of Energy and Environment* **7** (3), 282–291.
- Pandey, S. S., Singh, N. B., Shukla, S. P. & Tiwari, M. 2017 Removal of lead and copper from textile wastewater using egg shells. *Iranian Journal of Energy and Environment* **8** (3), 202–209.
- Ramezani, H., Azizi, S. N. & Cravotto, G. 2019 Improved removal of methylene blue on modified hierarchical zeolite Y: achieved by a ‘destructive-constructive’ method. *Green Processing and Synthesis* **8**, 730–741.
- Reghioua, A., Barkat, D., Jawad, A. H., Abdulhameed, A. S. & Khan, M. R. 2021a Synthesis of Schiff's base magnetic crosslinked chitosan-glyoxal/ZnO/Fe₃O₄ nanoparticles for enhanced adsorption of organic dye: modeling and mechanism study. *Sustainable Chemistry and Pharmacy* **20**, 100379. <https://doi.org/10.1016/j.scp.2021.100379>.
- Reghioua, A., Barkat, D., Jawad, A. H., Abdulhameed, A. S., Al-Kahtani, A. A. & AlOthman, Z. A. 2021b Parametric optimization by Box-Behnken design for synthesis of magnetic chitosan-benzil/ZnO/Fe₃O₄ nanocomposite and textile dye removal. *Journal of Environmental Chemical Engineering* **9** (3), 105166. <https://doi.org/10.1016/j.jece.2021.105166>.
- Rida, K., Bouraoui, S. & Hadnine, S. 2013 Adsorption of methylene blue from aqueous solution by kaolin and zeolite. *Applied Clay Science* **83–84**, 99–105.
- Sapawe, N., Jalil, A. A., Triwahyono, S., Shah, M. I. A., Jusoh, R., Salleh, N. F. M., Hameed, B. H. & Karim, A. H. 2013 Cost-effective microwave rapid synthesis of zeolite NaA for removal of methylene blue. *Chemical Engineering Journal* **229**, 388–398.
- Shirani, M., Semnani, A., Haddadi, H. & Habibollahi, S. 2014 Optimization of simultaneous removal of methylene blue, crystal violet, and fuchsin from aqueous solutions by magnetic nay zeolite composite. *Water, Air, & Soil Pollution* **225**, 1–15.
- Shukla, S. P., Singh, A., Dwivedi, L., Sharma, K., Bhargava, D. S., Shukla, R., Singh, N. B. & Yadav, V. P. 2014 Minimization of contact time for two-stage batch adsorber design using second-order kinetic model for adsorption of methylene blue (MB) on used tea leaves. *International Journal of Scientific and Innovative Research* **2**, 58–66.
- Singh, G. K., Singh, N. B., Shukla, S. P. & Markandeya. 2019 Remediation of COD and color from textile wastewater using dual stage electrocoagulation process. *SN Applied Sciences* **1**, 1000. <https://doi.org/10.1007/s42452-019-1046-7>.
- Solanki, P., Gupta, V. & Kulshrestha, R. 2010 Synthesis of zeolite from fly ash and removal of heavy metal ions from newly synthesized zeolite. *E-Journal of Chemistry* **7** (4), 1200–1205.
- Surip, S. N., Abdulhameed, A. S., Garba, Z. N., Syed-Hassan, S. S. A., Ismail, K. & Jawad, A. H. 2020 H₂SO₄-treated Malaysian low rank coal for methylene blue dye decolorization and cod reduction: optimization of adsorption and mechanism study. *Surfaces Interfaces* **21**, 100641. <https://doi.org/10.1016/j.surfin.2020.100641>.
- Thirunavukkarasu, A. & Nithya, R. 2020 Adsorption of acid orange 7 using green synthesized CaO/CeO₂ composite: an insight into kinetics, equilibrium, thermodynamics, mass transfer and statistical models. *Journal of the Taiwan Institute of Chemical Engineers* **111**, 44–62. <https://doi.org/10.1016/j.jtice.2020.04.007>.
- Tiwari, M., Shukla, S. P., Bhargava, D. S. & Kisku, G. C. 2013 Color removal potential of coal fly ash-a low cost adsorbent from aqueous solutions of disperse dyes used in textile mill through batch technique. *Our Earth* **10**, 5–8.
- Tiwari, M., Shukla, S. P., Mohan, D., Bhargava, D. S. & Kisku, G. C. 2015 Modified cenospheres as an adsorbent for the removal of disperse dyes. *Advances in Environmental Chemistry* **2015**, 1–8.
- USEPA T. 1990 *EPA Method 1311*. Washington, USA.
- Wang, L. 2013 Removal of disperse red dye by bamboo-based activated carbon: optimisation, kinetics and equilibrium. *Environmental Science and Pollution Research* **20** (7), 4635–4646.
- Yahia, M. B. & Sellaoui, L. 2020 Adsorptive removal of sunset yellow dye by biopolymers functionalized with (3-aminopropyltriethoxysilane): analytical investigation via advanced model. *Journal of Molecular Liquids* **312**, 113395. <https://doi.org/10.1016/j.molliq.2020.113395>.
- Zhang, L., Sellaoui, L., Franco, D., Dotto, G. L., Bajahzar, A., Belmabrouk, H., Bonilla-Petriciolet, A., Oliveira, M. L. S. & Li, Z. 2020 Adsorption of dyes brilliant blue, sunset yellow and tartrazine from aqueous solution on chitosan: analytical interpretation via multilayer statistical physics model. *Chemical Engineering Journal* **382**, 122952. <https://doi.org/10.1016/j.cej.2019.122952>.

First received 13 April 2021; accepted in revised form 24 May 2021. Available online 4 June 2021